2016 NDIA GROUND VEHICLE SYSTEMS ENGINEERING AND TECHNOLOGY SYMPOSIUM
MODELING & SIMULATION, TESTING AND VALIDATION (MSTV) TECHNICAL SESSION
AUGUST 2-4, 2016 - NOVI, MICHIGAN

Modeling of Landmine Loading of Armored Vehicles and Extension to Field Testing Assessment

David J. Stevens
Protection Engineering Consultants
San Antonio, TX

Matt A. Barsotti
Protection Engineering Consultants
Dripping Springs, TX

ABSTRACT

Protection Engineering Consultants (PEC) developed a soil model and landmine modeling strategy for LS-DYNA that resulted in excellent agreement with data from carefully controlled, precision tests. A traditional all-ALE approach and a less conventional all-SPH approach were evaluated, as well as hybrid formulations. Regardless of the modeling strategy used, the accuracy of landmine blast load predictions is strongly driven by the fidelity of the soil material model. PEC has developed a sandy soil model specifically for landmine simulations, which requires only two inputs: dry sand density and moisture content. Comparisons with data from two precision test series were exceptionally strong and the average error for predicted impulse was less than 2.5%, using a priori material parameter settings. This approach was employed to study the effects of disturbed soil above the landmine as occurs in live fire tests, where a hole is excavated, the landmine placed and the soil backfilled above the mine.

INTRODUCTION

As part of the United States Marine Corps (USMC) Mitigation of Blast Injuries through Modeling and Simulation project, Protection Engineering Consultants (PEC) developed a soil modeling strategy for LS-DYNA that resulted in excellent agreement with data from carefully controlled, precision tests. In developing this strategy, a traditional all-ALE (Arbitrary Lagrangian-Eulerian) approach and a less conventional all-SPH (Smooth Particle Hydrodynamics) approach were evaluated, as well as hybrid formulation strategies including combinations of ALE fluid and explosive materials with FEM (Finite Element Method), DEM (Discrete Element Method), or SPH soil.

Regardless of the modeling strategy used, the accuracy of landmine blast loads is strongly driven by the fidelity of the soil material model. Since most benchmark landmine tests have been performed on sandy soils of varying moisture contents, ranging from dry to fully saturated, and after a detailed literature survey and experimentation with the modeling approaches, PEC developed an independent approach to modeling sandy soil for landmine simulations. The sand model was based on test data for strength, compaction, and unloading modulus for different dry sand densities, and the density and yield strength were modified for added water content. This model requires only two inputs from the user: dry sand density and moisture content.

In numerical simulations of landmine detonations, the entire soil domain is often assumed to have the same density as specified in the test requirements. However, the procedure for placing the explosive charge in field tests results in a different soil density above the mine, due to backfilling the soil on top of the explosive using hand compaction. The effects of this density change on the resulting loads were studied.

SANDY SOIL MATERIAL MODEL DEVELOPMENT

The accuracy of landmine blast load predictions appears to be strongly driven by the fidelity of the soil material model, regardless of the modeling strategy (FEM, ALE, SPH, etc). Since many benchmark landmine tests have been performed on sandy soils of varying moisture contents, ranging from dry to fully saturated, soil modeling efforts were focused on sand.

A detailed literature survey was conducted and, while a detailed review is beyond the scope of this paper, key research included noted references from the US Army Engineer Research and Development Center (ERDC), Army Research Laboratory (ARL), US Army Tank-Automotive

Material reported in this paper which are results of Contract # M67854-13-C-0225 have been cleared for public release by the USMC

Research Development and Engineering Center (TARDEC), Aberdeen Proving Ground (APG), Defense Nuclear Agency, Canadian Defence Research Establishment Suffield (DRES), Norwegian Geotechnical Institute (NGI), Southwest Research Institute (SwRI), Ernst Mach Institute (EMI), Clemson University (CU), Sandia National Laboratories (SNL), Schwer Engineering and Consulting Services, and the Wright Laboratory Flight Dynamics A full literature review may be found in the USMC MBI report (1).

An independent approach to modeling sandy soil was developed, using *a priori* definitions determined by normal soil constitutive properties, without requiring recourse to *post hoc* material tuning. Conceptually, the approach is similar to the Kerley method described by Anderson (2); however, alignment with Kerley on various specific points is unknown.

Baseline Sand Properties

The baseline material properties used to represent sandy soils were derived from two primary sources. The majority of the properties were based upon Sjobo sand, as characterized by Laine & Sandvik (3), which included compaction, strength, and modulus. Yield strength properties for varying levels of saturation were derived from Kerley (4, 5). For dry sand, Laine and Kerley show nominal agreement.

Dry Density Modifications

Modification of the Sjobo properties to represent alternate dry densities was relatively straightforward. It was assumed that the terminal density and modulus of fully compacted sand were nominally the same for different species, i.e., that of pure quartz (ρ = 2,650 kg/m^3). Variations in dry density can be influenced by particulate gradation, particulate sphericity, and material consolidation arising from tamping or vibration. The ratio of the loose and terminal density for Sjobo sand indicates a void fraction of approximately 37%. For higher or lower dry sand densities, the pressure-density curve was either compressed or dilated from the left end while leaving the terminal density unaltered.

Saturation Modifications

Two modifications were made to account for an arbitrary level of saturation. First, the yield strength was modified per Kerley (5). The initial slope of the yield surface remained that of dry Sjobo sand, but the flat-line strength plateau was adjusted. Secondly, the compaction curve was separated into two components. The first was a semi-parabolic load curve representing pressure versus volumetric strain for the void space compaction of the dry soil skeleton, up to the terminal lockup point. The second part represented the terminal lockup in which no voids remain in the sand (effectively the bulk modulus of quartz). A third component for water was defined by the Gruneisen equation of state, which defines a semi-parabolic curve that has a vertical asymptote at a volumetric strain of ~0.5. These three components were merged into a three-spring model, depicted by the simplified one-dimensional schematic of Figure 1. Two of the spring elements (K_W & K_V) were nonlinear, and the gauge length of each element was determined based upon the void fraction and saturation level of the soil. Using the three-spring relationship, the compaction curve for any sand can be defined by calculating the net spring resistance across the full range of compression strains. For the case of fully saturated sand, the initial modulus produced by this spring system matches that given by the Wood equation (6).

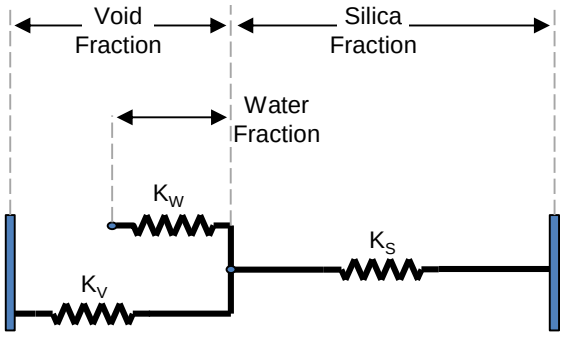

Figure 1. Element Schematic of Three-Spring Compaction Model

The bounding behavior of the three-spring model was verified by calculating the net compression resistance for pure Sjobo sand and pure water, both of which overlay their respective reference curves correctly. When applied to varying saturation levels, the three-spring model produced compression curves that demonstrated the expected water lockup behavior, plotted for clarity in engineering strain (Figure 2). The compaction curves were defined throughout the full volumetric strain regime, as is required for landmine models in which the material in immediate contact with the charge is compressed to the terminal quartz limit.

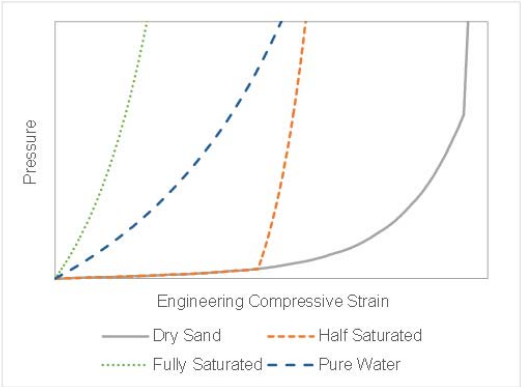

Figure 2. Typical Compaction Curves for Sand at Varying Levels of Saturation

LS-DYNA Modeling

In LS-DYNA, the soil was modeled using two keywords. The elastic properties and yield strength were modeled with *MAT_PSEUDO_TENSOR. The strength versus pressure yield surface was defined as a simple bilinear curve with a maximum strength plateau per Kerley. The compaction behavior and unloading modulus were defined using the equation of state *EOS_TABULATED_COMPACTION, which was populated per the three-spring methodology described above.

MODELING STRATEGIES

A number of different numerical modeling strategies for simulating landmine detonations were considered; see Figure 3. ALE and SPH formulations were both used to model the complete mine problem, including soil, air, and explosive. Three hybrid approaches were also considered, which separated the air/explosive from the soil, using ALE for the former and FEM, SPH, or DEM for the latter.

		Soil Formulation			
		ALE	FEM	SPH	DEM
HE & Air Formulation	ALE	✓	✓	✓	✓
	FEM				
	SPH			✓	
	DEM				

Figure 3. Combinations of Modeling Strategies

The full ALE approach was taken as the baseline for the effort. The two primary shortfalls of the ALE formulation include the need for a large domain that engulfs the target vehicle undercarriage and the need for fluid-structure interaction (FSI) coupling algorithms. The former produces a computational burden on the simulation, while the latter can be plagued by leakage and stability issues.

The full SPH approach avoids the ALE domain size requirements, since separate particles can transit unlimited distances without an intervening fluid containment mesh. It also eliminates complications arising from FSI, since normal Lagrangian contacts may be used for mine-vehicle interactions. Drawbacks include a higher computational expense than ALE, in part because the code must repeatedly parse the model domain to determine which particles are in proximity to one another. The comparative cost is further exacerbated because SPH typically requires a finer discretization to obtain similar accuracy; it is not uncommon to employ an 8:1 ratio in 3D models. Finally, the drastic difference in density between air and soil requires the use of particle-to-particle contact at the air-soil interface, which can be the source of significant instability.

The hybrid ALE-SPH approach represented soil near the explosive charge with SPH particles, while the explosive and air constituents were modeled using ALE. This mitigated the SPH computational expense and was considered the most organic representation of the granular nature of the soil material and the fluid nature of air and explosive products. Soil far from the charge was represented with finite element bricks. The ALE explosive loaded the SPH soil particles through FSI penalty coupling.

The hybrid ALE-FEM approach was inspired by literature that featured the modeling of soil with eroding finite elements (7, 8). Within LS-DYNA, the eroding elements can be either converted into deleted nodes or into SPH particles. The deleted node approach can lead to a fictitious loss of soil volume which reduces the confinement on the expanding gas products. Converting deleted elements to SPH particles offered a more elegant solution that was capable of retaining soil volume while still adapting to extreme deformations. This LS-DYNA option was nominally comparable to the manner in which EPIC converts distorted finite elements into particles (8). In practice, however, the LS-DYNA conversion proved numerically unstable. The explosive and air were modeled with ALE materials, and the FSI coupling during erosion was numerically fragile. As the code attempted to transition the explosive coupling from the soil finite elements to the newly-formed soil SPH particles, error terminations often resulted. At present, this capability within LS-DYNA seems to lack the necessary maturity for reliable use.

The hybrid ALE-DEM approach was considered since the discrete element method (DEM) has risen in popularity over the last several years. Some codes, such as IMPETUS, model landmines exclusively with DEM (9). Yet DEM differs notably from ALE, FEM, and SPH, all of which rely on continuum mechanics to define materials with a combination of strength model and compaction model. DEM consists instead of a collection of rigid mass particles that interact via spring-damper contact definitions. Tuning a DEM definition to accurately represent landmine behavior requires a series of landmine tests conducted on that specific soil. Practically speaking, however, there is no intrinsic bridge from material properties (derived from laboratory tests) to landmine predictions. After initial trials and material property considerations, pursuit of DEM was suspended.

MODELS OF SOIL EXPANSION

The Defence Research Establishment Suffield (DRES) in Alberta Canada carried out an experimental test program aimed at studying the basic explosion physics of shallow-

buried charges (10) (11). The test series involved the detonation of C-4 explosive disks weighing nominally 100-g when buried at various depths within a barrel of sand.

LS-DYNA was used to simulate these soil expansion tests with the ALE, SPH, and hybrid ALE-SPH strategies for 3-cm and 8-cm depth of burial (DOB) cases, using a 3-dimensional, quarter-symmetry computational domain. Figure 4 shows experimental and ALE model soil bubble profiles for the 8-cm DOB (left) and a comparison of expansion trends for both DOB.

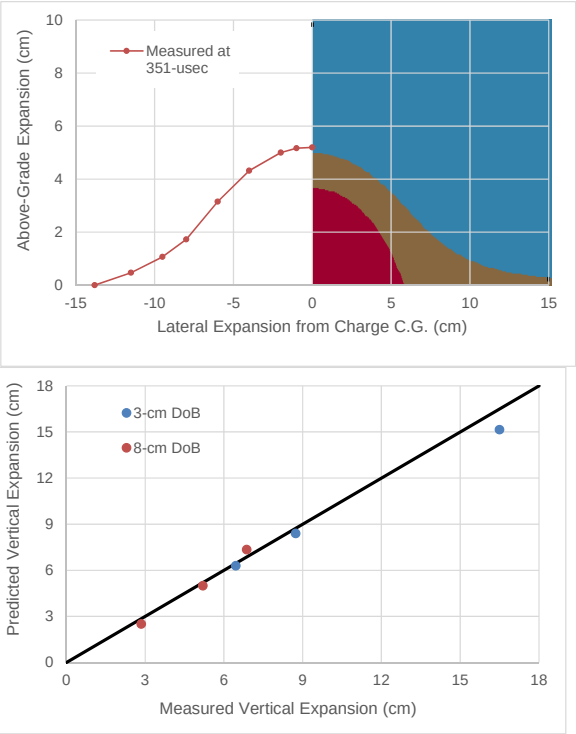

Figure 4. 8-cm DOB Soil Expansion Simulation for ALE Modeling Strategy, PEC Soil Model; Measurements Adapted from (17)

The pure SPH simulations were carried out with a 3-dimensional, quarter-symmetry computational domain. Typical particle spacing was 1.5-mm, or one-half that of the comparable ALE model. Due to identified numerical instabilities involving SPH air particles, air was neglected during these simulations. Figure 5 shows experimental and model soil bubble profiles for the 8-cm DOB (left) and a comparison of expansion trends for both DOB. In comparing the ALE trend of Figure 4 and the SPH trend of Figure 5, it is clear that the SPH modeling strategy is less accurate and seems to enhance the ALE error trends, alternately yielding under- and over-predicted expansions.

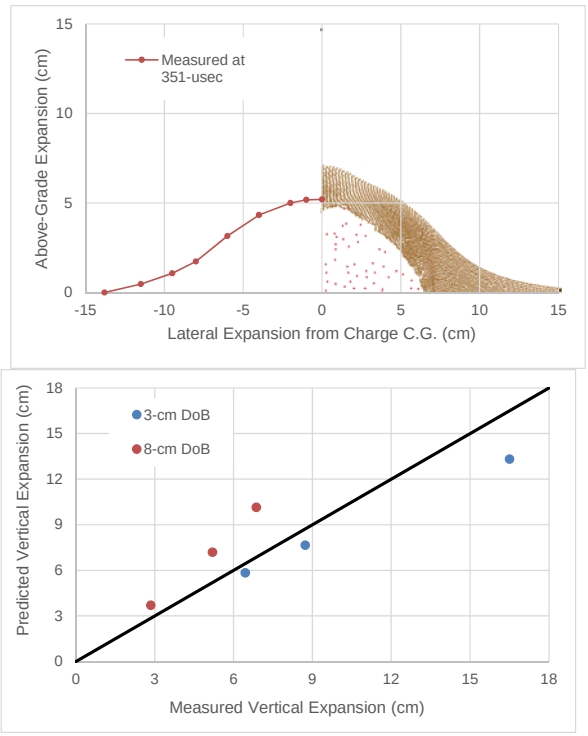

Figure 5. 8-cm DOB Soil Expansion Simulation for SPH Modeling Strategy; Measurements Adapted from (17)

The hybrid ALE-SPH simulations were carried out with a 3-dimensional, quarter-symmetry computational domain. Typical SPH particle spacing was 1.5-mm, and the typical ALE element size was 3-mm (i.e., an 8-to-1 SPH-to-ALE ratio was employed, where 8 SPH particles could fit into a single ALE element volume). Figure 6 shows experimental and model soil bubble profiles for the 8-cm DOB (left) and a comparison of expansion trends for both DOB. The results show that the hybrid ALE-SPH formulation always under-predicted vertical expansion, likely due to progressive leakage of the detonation products through the soil cap, which could not be entirely eliminated.

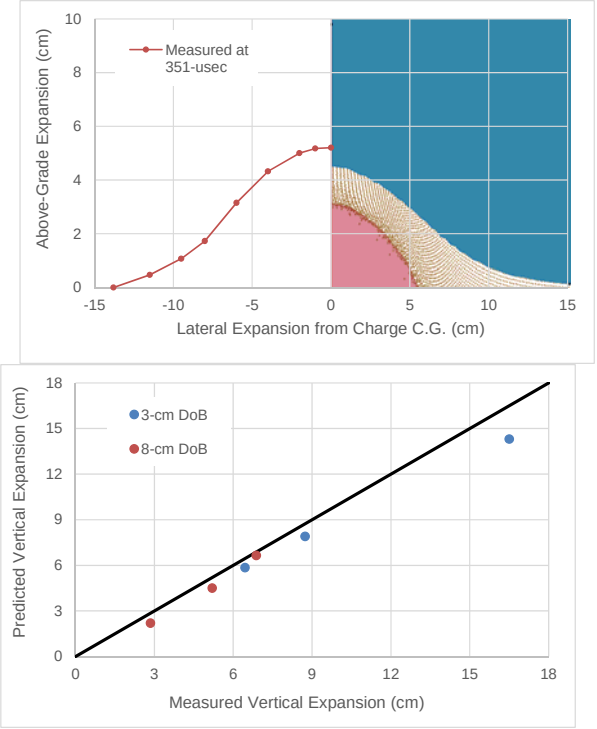

Figure 6. 8-cm DOB Soil Expansion Simulation for Hybrid SPH-ALE Modeling Strategy; Measurements Adapted from (17)

MODELS OF TARGET IMPACT

LS-DYNA was used to simulate two series of landmine plate impact tests, which were conducted by the Ernst Mach Institute (EMI), per Anderson (2), and the Army Research Laboratory (ARL), Aberdeen Proving Ground (APG), per Skaggs (12). These test series offered a range of charge sizes, plate shapes, and soil saturation conditions, of which a subset was chosen to evaluate the various LS-DYNA modeling strategies and the PEC sandy soil material modeling approach. In each case, imparted momentum and velocity histories were recorded for the target plate during each simulation for comparison with reported values.

ALE Models for Partially Saturated EMI Tests

The ALE modeling strategy was investigated for the EMI flat plate, 90-deg bent plate, and 120-deg bent plate impact scenarios using a 3-dimensional, quarter-symmetry computational domain. In these tests, sand with different saturation levels was placed in a sonotube (hollow cardboard tube); the diameter and depth of the tube were 0.63-m and 0.85-m, respectively. The depth of burial for the 0.674-kg Comp-B charge was 0.05-m. The steel plate was 0.06-m thick and approximately 0.8-m square, depending on the bend; the weight was 300-kg. The ALE domain in the region of the sonotube and plate was modeled with 5-mm bricks (10 elements through soil cap), and it dilated to progressively larger elements outside this region. It extended well beyond the sonotube radius and the target height to allow soil expansion and explosive circulation. The plate-to-soil friction coefficient was 0.2, as found in the literature.

Following the development of the three-spring soil model, the material properties were automatically calculated using two *a priori* values: the dry density of the EMI test soil and the water content of the specific test case. Reports by Anderson, et al, listed the soil conditions during testing using moisture content and gross density (2, 13). The as-received sand was reported at 1.37 g/cm^3 with a moisture content of 7%; water was added to obtain two additional moisture content levels of 14% and 22%. The dry density of the material was calculated as 1.28 g/cm^3. Using the dry density and moisture contents for each species, compaction and strength curves were generated for each material, which were used for the EMI models of test series 1, 3, 4, 5, and 6. Soil expansion renderings for the EMI 120-deg plate and flat plate are shown in Figures 7 and 8.

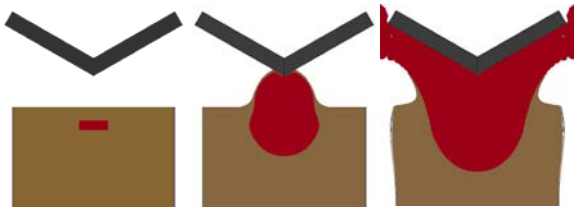

Figure 7. ALE Response Evolution for EMI 120-deg Bent Plate Impact Simulation

Figure 8. ALE Response Evolution for EMI Flat Plate Impact Simulation

Model results for five EMI cases are summarized and compared with predictions from prior researchers in Figure 9. The grey bars represent the average EMI experimental impulses, and the corresponding error bars show the experimental spread. The blue bars give the results obtained with PEC soil model, while the green bars show the predictions made with CTH by SwRI and with LS-DYNA by Schwer (2, 13, 14).

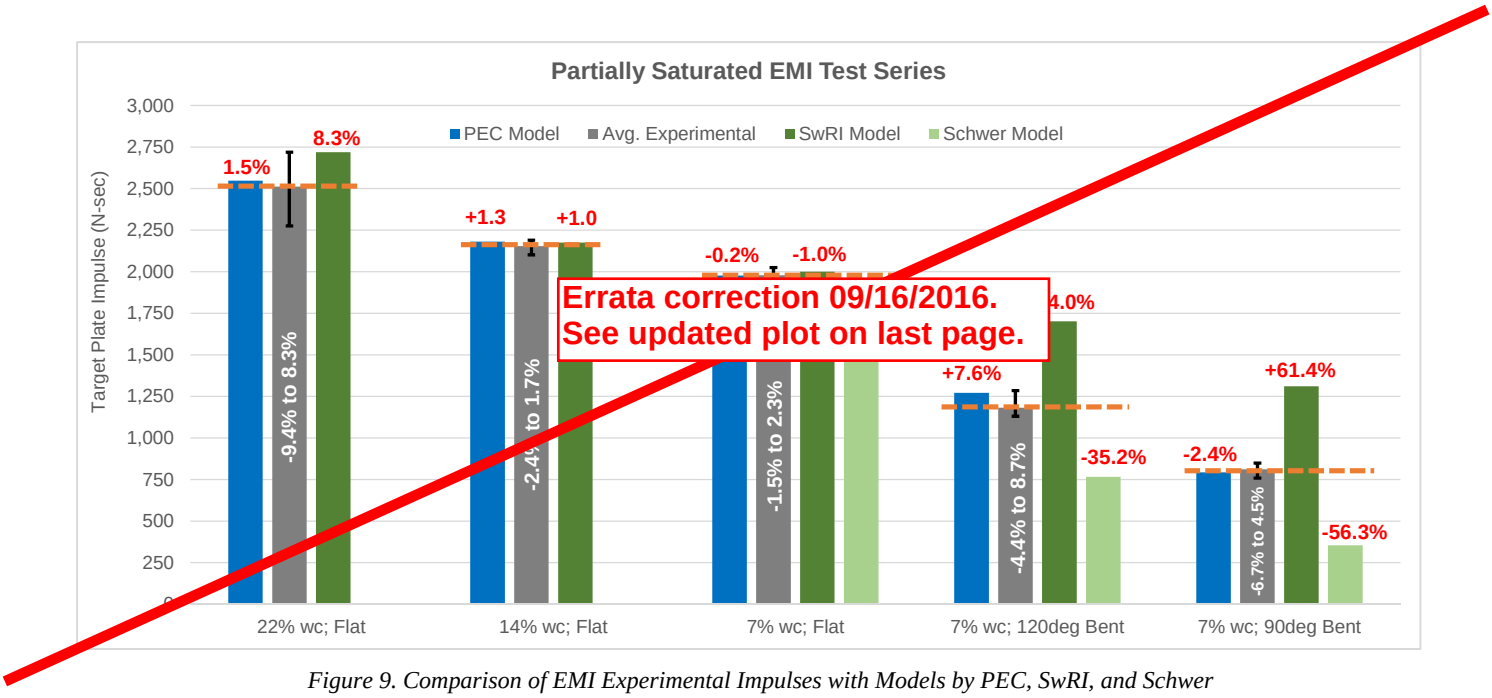

Figure 9. Comparison of EMI Experimental Impulses with Models by PEC, SwRI, and Schwer

A comparison of the trends reveals that SwRI and Schwer predicted the loading well for flat plate scenarios, but they diverge from experiment when V-shaped targets were introduced. CTH predictions from SwRI tended to over-predict impulse for the V-plates, while LS-DYNA simulations by Schwer tended to under-predict. In general, flat plate impulses seem to be easier to match, while the V-plates present a harder challenge and are more sensitive to material model and/or code differences.

The PEC model in LS-DYNA matched the loads for the bent plates well, falling within the error bars of the experimental tests in all cases. The average error across all cases, including both flat and V-shaped targets, was under 3%. Irrespective of geometry, the PEC soil model appears to accurately replicate the EMI tests without *post hoc* material tuning.

A comparison of the impulses for the three test cases with 7% water content is shown in Figure 10, where the horizontal lines show the EMI experimental averages and bounds. Trends for the other test cases showed similar correspondence.

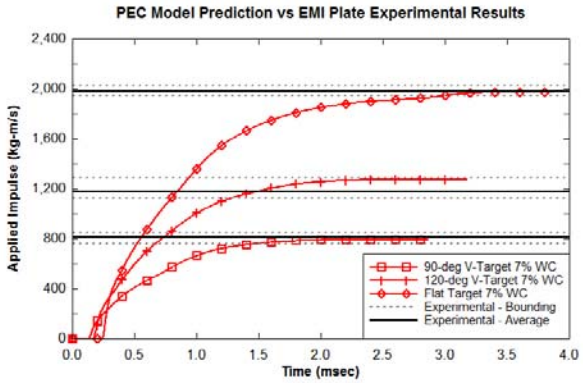

Figure 10. ALE Imparted Momentum for EMI Tests with 7% Water Content, PEC Soil Model

ALE Models for Fully Saturated VIMF Tests

The ALE models for the VIMF tests used an axisymmetric domain, because only a flat plate target was used and the soil domain was large. The target plate radius was modeled such that the axisymmetric plate would have the same surface area as the rectangular VIMF target. The ALE domain in the saturated test region (within the pool liner) was modeled with 5-mm bricks. It dilated to progressively larger elements outside this region.

Two cases from the experiment matrix were modeled. Both tests featured a charge in fully saturated sand. As with

the EMI models, properties for the PEC three-spring compaction soil model were set *a priori* using two values: the dry density of the VIMF test soil and the fully-saturated water content. The dry density was 1.49 g/cm^3 and the fully saturated density at 1.91 g/cm^3 (16).

The PEC soil model matched the loads for both tests well, with an average error of just under 2% (since the actual experimental values in the limited distribution ARL report have not been published in the open literature, they were omitted from this paper and the impulse comparisons are relative). In contrast with the EMI test series, it should be noted that the charge size and impulse loads were an order of magnitude larger, and the soil was fully saturated, thus illustrating the versatility of the PEC approach across a range of saturation conditions and load severity.

SPH Models for Partially Saturated EMI Tests

The SPH models for the EMI tests used a quarter-symmetric 3-dimensional domain. SPH particles were used in a limited region of the domain due to computational costs. The SPH domain was coupled to an FEM brick domain outside this area, which made up the balance of the Sonotube volume. Models were run with both the default and renormalized particle formulations, but typically the default was used.

Trials of the SPH approach showed an instability related to the inclusion of air particles. The drastic difference in mass density between air and soil/high-explosive required the use of a particle-to-particle contact at the air-soil interface. In some cases this coupling worked well (Figure 11). As the SPH air particles become unstable, they shoot off at excessively high velocities through the computational domain, causing additional instabilities as the rogue particles collide with stable neighboring particles (Figure 12). In simulations that ran long enough before the onset of shooting particles, the air contribution was found to be small and to take place relatively early in time. Over longer simulation times with ALE, it was estimated that air contributed less than 3% of the total momentum. In light of the minor contribution and the intractable stability issues, air was neglected in the SPH plate impact models.

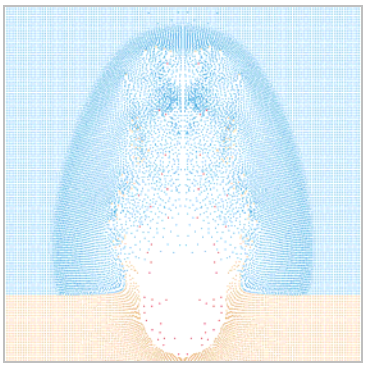

Figure 11. Stable SPH Air to Soil Particle Contact

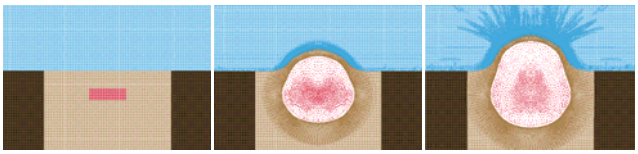

Figure 12. Unstable SPH Air to Soil Particle Contact Caused by Shooting Rogue Particles

Unlike the ALE formulation, the SPH formulation was found to generally under-predict peak imparted momentum; see Figure 13. Errors were approximately 15-percent or less for all target plate configurations. From a standpoint of computational expense, the SPH simulations were markedly more costly than the ALE simulations.

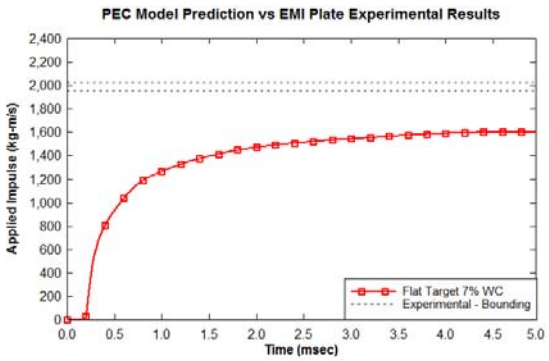

Figure 13. SPH Imparted Momentum for EMI Flat Plate Test with 7% Water Content, PEC Soil Model

Hybrid ALE-SPH Models of EMI Tests

Preliminary ALE-SPH hybrid models were constructed for the flat plate and 90-deg bent plate EMI tests. The ALE domain used 5-mm elements that contained air, explosive, and soil materials. The soil was represented with SPH particles in the vicinity of the buried charge, and the typical particle spacing was 2.5-mm (i.e., 8-to-1 ratio of SPH particles to a single ALE element). The soil transitioned to a

FEM brick representation at a depth of 200-mm from the soil surface.

Numerical instabilities plagued the hybrid simulations, resulting in premature terminations that were unresolvable. A unique challenge associated with the hybrid ALE-SPH approach involved the FSI coupling algorithms required for the ALE-to-SPH interaction. Comparison of the incomplete impulse histories (not shown) with the pure SPH models showed worse under-prediction. Owing to the complexity, computational expense, and poor results, development of the hybrid approach was eventually suspended.

Influence of ALE Mesh Discretization

The effects of ALE mesh size were examined to ensure that discretization error was not adversely influencing the results. Since the EMI tests used smaller charge sizes and shallower burial depths than the VIMF tests, the flat plate 7% water content case was selected for evaluation. A set of simplified 2D axisymmetric ALE models were constructed with the same cross-sectional dimensions as the 3D models previously discussed. Mesh sizes of 10-mm, 6-mm, 5-mm, and 4-mm were evaluated. The axisymmetric target radius was set to give a circular area equivalent to the rectangular test plate. Because the virtual target was fixed in space and massless, factors like inertial acceleration, gravity force, and resistance from air above the target were not included. As such, the load histories measured in these models are comparable to one another for evaluating discretization effects, but they are not strictly comparable to the prior 3D inertial plate models.

Early loading and the time of arrival showed some mesh dependence, but the total impulse after 10 msec was not greatly affected by mesh size (Figure 14). The trend for total impulse proved to be fairly flat, with no clear convergence or divergence. It showed only a slight oscillation around the average value. The impulse range fell within +/-0.75% of the mean. This brief examination indicated that the use of 5-mm ALE meshes in the 3D models was appropriate, and that the mesh discretization errors were not unduly affecting the model results.

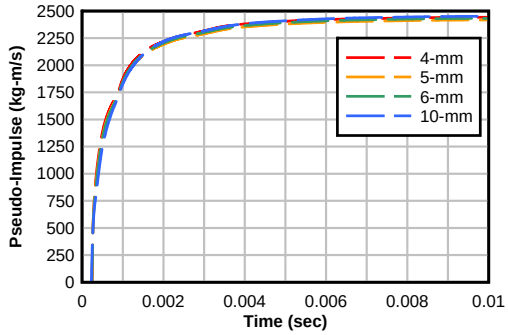

Figure 14. Impulse Histories for Different ALE Element Sizes, EMI Flat Plate 7% Water Content

EVALUATION OF FIELD TEST CONDITIONS

In field and live fire tests, the procedure for placing the explosive charge will typically result in a different density for the soil directly above the explosive. The soil bed is often placed in layers that are mechanically compacted; density and moisture content measurements are made and recorded for each lift. Prior to testing, the explosive technician will manually dig the hole, put the spoil in a container, place and arm the explosive, and then backfill the spoil on top of the explosive. The water content of the spoil will change while exposed to the air and the compaction of the replaced soil above the explosive is generally done carefully by hand, so as not to disturb the detonator and firing line. As shown by the three sets of data on the left side of Figure 9 (22%, 14%, and 7% wc), water content and, hence, density significantly affect the impulse that is delivered to the flat plates.

As a part of a preliminary study to explore the effect of reduced soil density and water content in the soil directly above the explosive in a live fire test, a number of simulations of the flat plate EMI precision tests were performed. The quarter symmetry LS-DYNA model is shown in Figure 15, where the soil above the explosive has a reduced density and water content.

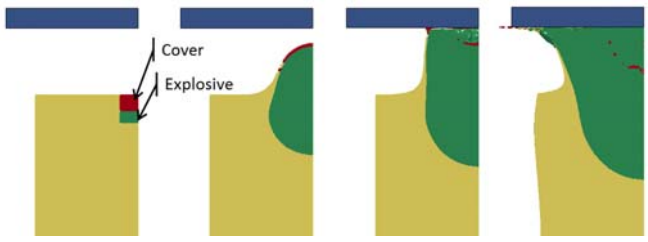

Figure 15. Reduced Density and Water Content above Explosive, EMI Flat Plate

The results for a cover thickness of 5-cm is shown in the top of Table 1. Somewhat counter-intuitively, there was

little variation with applied impulse as the soil density and water content above the explosive were both decreased. This suggests that the soil around and below the explosive plays a very large role in determining the impulse that is generated; the surrounding soil acts as a spongy layer to confine the detonation and propel the soil above the explosive upwards; denser and stronger soils provide more confinement and increase the impulse load. The lighter density soil above the explosive achieves higher velocity so that the overall impulse from the soil and explosive byproducts remains relatively unchanged.

For thinner cover thicknesses, the explosive byproducts and pressure may leak through the soil cap earlier in the event, thus decreasing the velocity of soil above the explosive. To explore this, the cover layer was decreased to 2.5-cm and the same set of properties for the soil above and surrounding the explosive was evaluated. The results are shown in the bottom of Table 2. Again, little variation in applied impulse is observed.

The counter-intuitive conclusion of this preliminary investigation is that the density and moisture content of the soil above the explosive have very little effect on the delivered impulse.

Density, kg/m^3	Water Content, %	Density, kg/m^3	Water Content, %	Impulse, N-sec
Soil Bed		**Soil Above Mine**		
5 cm Cover				
1670	22	1670	22	2544
1670	22	1490	14	2528
1670	22	1370	7	2512
2.5 cm Cover				
1670	22	1670	22	2112
1670	22	1490	14	2108
1670	22	1370	7	2056

Table 1. Impulse Variation with Density and Water Content

MATERIAL PROPERTIES AND ACCURACY

During the evaluations of the various modeling strategies and the development of the PEC sandy soil material modeling approach, several observations were made regarding the relationship of soil material properties and prediction accuracy. It was noted that density has a strong effect on impulse, while soil strength proved to be much milder.

The most important observation was the criticality of compression properties of the material. The effects of the compression curve were more important than those of material density. Phenomenologically, the rapidly expanding explosive byproducts are contained, at least in a transient sense, by the spongy soil surrounding them. The degree of compliance in this pseudo container determines how much energy is immediately absorbed from the expanding explosive byproducts. Where the soil is fully saturated, and therefore proves less spongy and more confining, the sides and bottom of this soil container allow far less volume expansion, thereby driving the explosion energy upward with stronger directional bias.

Simplifying assumptions regarding the compression curve may be partly responsible for predictive inaccuracies in some of the prior modeling efforts surveyed in the literature. Adverse assumptions may include errors in estimating dry density, errors in defining the point of water lockup, linear assumptions regarding water compression, or failures to carry the compression curve to sufficiently high strains and related compression modulus.

Qualitatively, the experiences of this effort suggest the following rank ordering for material properties as they relate to predicted impulse accuracy:

1. Compression curve
2. Density
3. Yield strength curve
4. Plate friction

CONCLUSIONS

Several LS-DYNA modeling strategies were evaluated for simulating landmine explosions, including ALE, SPH, hybrid ALE-SPH, eroding FEM to SPH, and DEM. Evaluations included the examination of initial soil bubble expansion and the imparted impulse on flat and V-shaped plate targets. The all-ALE formulation clearly produced the most accurate predictions of soil bubble expansion and target impulse. While the all-SPH strategy was viable, it was computationally expensive and tended to under-predict impulse. Comparable accuracy to ALE may be possible, but likely only with even finer meshing and greater computational cost. The hybrid ALE-SPH strategy proved to be the most complicated and least accurate. Attempts with an eroding FEM to SPH strategy proved unstable and unreliable. The DEM approach was examined but not heavily investigated due to its inability to allow *a priori* constitutive property definition from soil material properties.

A notable accomplishment of this effort was the development of a generalized sandy soil model using a three-spring approach for defining the material compaction curve. A full material model definition is based on only two *a priori* input values: dry density and saturation percentage. The use of the PEC sandy soil model showed high accuracy across a range of soil saturation levels, target shapes, and for widely varying charge sizes. No *post hoc* material tuning was employed to improve the correlation to experimental results. The average error was under 3%, with V-plates

showing around 5% error, all of which were within the experimental data scatter. Accuracy was found to depend heavily upon the compression curve and the density of the soil, while material strength proved to be of secondary importance.

An investigation was performed of field test conditions in which the soil above the explosive has reduced density and water content, as compared to the soil surrounding and below the explosive. The numerical results showed that the density and water content have little effect on the delivered impulse, a somewhat non-intuitive but rational finding.

REFERENCES

[1] **Barsotti, Matt, Sammarco, Eric and Stevens, David J.** *Mitigation of Blast Injuries Through Modeling and Simulation: Task 1 Report: Soil and Explosive Modeling.* Quantico : United States Marine Corps MARCORSYSCOM, via Protection Engineering Consultants, 2015.

[2] **Anderson, Charles E., et al., et al.** *18.12544/011: Mine-Blast Loading: Experiments and Simulations.* Southwest Research Institute. Herndon : US Army Tank-Automotive Research, Development and Engineering Center, 2010. 18.12544/011.

[3] *Derivation of Mechanical Properties for Sand.* **Laine, Leo and Sandvik, Andreas.** Singapore : CI-Premier PTE LTD, 2001. 4th Asia-Pacific Conference on Shock and Impact Loads on Structures. pp. 361-368.

[4] **Kerley, Gerald I.** *Documentation of Data on Sandia ANEOS Library File.* Albuquerque : Sandia National Laboratories, 2001.

[5] **Kerley, G.I.** *ARL-CR-461: Numerical Modeling of Buried Mine Explosions.* s.l. : Aberdeen Proving Ground, 2001.

[6] **Blouin, S E and Kwang, J K.** *Undrained Compressibility of Saturated Soil: Report DNA-TR-87-42.* Washington, DC : Defense Nuclear Agency, 1984. DNA-TR-87-42.

[7] *ARL-RP-98: Simulating the Blast of Buried Mines on Lightweight Vehicle Hulls.* **Cheeseman, Bryan A., et al., et al.** Monterey, CA : Army Research Laboratory, 2005. 15th Annual Ground Vehicle Survivability Symposium. ARL-RP-98.

[8] **Moral, Ramon J., Danielson, Kent T. and Ehrgott, John Q. Jr.** *ERDC/GSL TR-10-27: Tactical Wheeled Vehicle Survivability: Comparison of Explosive-Soil-Air-Structure Simulations to Experiments Using the Impulse Measurement Device.* Geotechnical and Structures Laboratory, Engineer Research and Development Center. Vicksburg, MS : US Army Corps of Engineers, 2010. ERDC/GSL TR-10-27.

[9] *Discrete Particle Approach to Simulate the Combined Effect of Blast and Sand Impact Loading of Steel Plates.* **Borvik, T., et al., et al.** 59, s.l. : Elsevier Ltd., March 2, 2011, Journal of the Mechanics and Physics of Solids, pp. 940-958.

[10] **Bergeron, D, Walker, R and Coffey, C.** *Report 668: Detonation of 100-gram Anti-Personnel Mine Surrogate Charges in Sand: a Test Case for Computer Code Validation.* Alberta : Defense Research Establishment, Suffield, 1998.

[11] *A Computational Analysis of Detonation of Buried Mines.* **Grujicic, M., Pandurangan, B. and Cheeseman, B.A.** s.l. : Brill, September 20, 2005, Multidiscipline Modeling in Mat. and Str., pp. 1-26.

[12] **Skaggs, R. Reed, Gault, William and Taylor, Leslie C.** *ARL-TN-250: Vertical Impulse Measurements of Mines Buried in Saturated Sand.* Weapons and Materials Research Directorate. Aberdeen Proving Ground, MD : U.S. Army Research Laboratory, 2006. ARL-TN-250.

[13] *Mine Blast Loading: Experiments and Simulation.* **Anderson, Charles E, et al., et al.** Herndon, VA : ARL Research in Ballistic Protection Technologies Workshop, 2010.

[14] **Schwer, Len.** *Simulations of SwRI Buried Charge Experiments.* Schwer Engineering & Consulting Services, SwRI. Windsor, CA : s.n., 2012.

Correction:

September 16, 2016

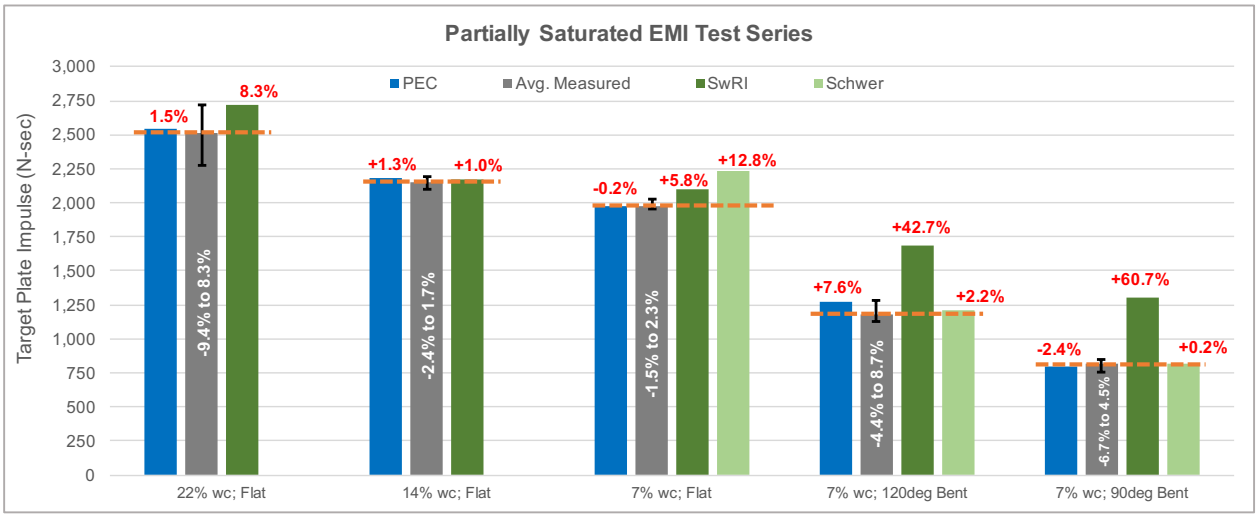

REVISED Figure 9. Comparison of EMI Experimental Impulses with Models by PEC, SwRI, and Schwer [15]

[15] Schwer, L. and T. Slavik. *Buried Charge Engineering Model: Verification and Validation.* in 9th European LS-DYNA Conference. 2013.